

Giant switchable Rashba effect in oxide heterostructures

Zhicheng Zhong¹, Liang Si¹, Qinfang Zhang², Wei-Guo Yin³, Seiji Yunoki⁴ and Karsten Held¹

¹*Institute of Solid State Physics, Vienna University of Technology, A-1040 Vienna, Austria*

²*Key Laboratory for Advanced Technology in Environmental Protection of Jiangsu Province, Yancheng Institute of Technology, China*

³*Condensed Matter Physics and Materials Science Department, Brookhaven National Laboratory, Upton, New York 11973, USA*

⁴*Computational Condensed Matter Physics Laboratory, RIKEN, Wako, Saitama 351-I0198, Japan*

One of the most fundamental phenomena and a reminder of the electron's relativistic nature is the Rashba spin splitting for broken inversion symmetry. Usually this splitting is a tiny relativistic correction, hardly discernible in experiment. Interfacing a ferroelectric, BaTiO₃, and a heavy 5d metal with a large spin-orbit coupling, Ba(Os,Ir)O₃, we show that giant Rashba spin splittings are indeed possible and even fully controllable by an external electric field. Based on density functional theory and a microscopic tight binding understanding, we conclude that the electric field is amplified and stored as a ferroelectric Ti-O distortion which, through the network of oxygen octahedra, also induces a large Os-O distortion. The BaTiO₃/BaOsO₃ heterostructure is hence the ideal test station for studying the fundamentals of the Rashba effect. It allows intriguing application such as the Datta-Das transistor to operate at room temperature.

PACS numbers: 73.20.-r, 73.21.-b, 79.60.Jv

An electric field control of the spin degree of freedom is the key to spintronics and magnetoelectrics [1]. In the prototypical spintronic device, the Datta-Das spin transistor [2], an electric field tunes the Rashba spin splitting and with that the spin precession frequency. The precession in turn controls the spin polarized current between two ferromagnetic leads. Microscopically, the Rashba spin splitting originates from the spin orbit coupling (SOC) in a two dimensional electron gas (2DEG) with broken inversion symmetry perpendicular to the 2DEG plane [3, 4]. It has been observed for metal surfaces [5, 6], semiconductor and oxide heterostructures [7–12], and even in polar bulk materials [13]. The Rashba effect splits parabolic bands into two subbands with opposite spin and energy-momentum dispersions $E^\pm(\mathbf{k}) = (\hbar^2\mathbf{k}^2/2m^*) \pm \alpha_R|\mathbf{k}|$. Here, m^* is the effective mass, \mathbf{k} the wave vector in the 2DEG plane, and α_R the Rashba coefficient which depends on the strength of SOC and inversion asymmetry. An electric field modulates this inversion asymmetry and consequently the Rashba spin splittings. The electric-field induced change of α_R is however weak: up to 10^{-2}eV\AA in semiconductor [7] or 3d transition metal oxide heterostructures [8–10]. A large, electric-field tunable Rashba effects are also much sought-after in the research area of topological insulators [14–16].

Giant Rashba effects with α_R of the order of 1eV\AA have been reported for metal surfaces [6], Bi adlayers [17] and bulk polar materials BiTeI [13, 18]. The large α_R here relies on the surface or interface structural asymmetry, which is hardly changes in an external electric field. To enhance the tunability by an electric field, Di Sante *et al.* [19] hence suggested a ferroelectric semiconductor GeTe. For GeTe, an external electric field switches between paraelectric and ferroelectric phase, breaking in-

version symmetry and tuning on the Rashba spin splitting. At first glance, this perfectly realizes an electric field control of a giant Rashba effect. However, there is an intrinsic difficulty: A single material cannot be both, a conductor with large Rashba spin splitting and a ferroelectric which necessarily is insulating.

In this letter, we propose to realize a giant switchable Rashba effect by heterostructures sandwiching a thin metallic film of heavy elements in-between ferroelectric insulators, see Fig. 1. The thin film provides a 2DEG with strong SOC, while the inversion asymmetry is induced by the structural distortion of the ferroelectrics and tunable by an electric field. As a prime example, we study a heterostructure of transition metals oxides, BaOsO₃/BaTiO₃. BaTiO₃ is a well-established ferroelectric [20]. It has a simple high-temperature perovskite structure, with Ba atoms at the edges, a Ti atom at the center and the O atoms at the faces of a cube. Such a structure has an inversion symmetry center at the Ti site. At room temperature, inversion symmetry is broken since a ferroelectric structural distortion occurs with a sizable Ti-O displacement $z_{\text{Ti-O}}$ along one of the the cubic axes. BaOsO₃ has been recently synthesized; it is a metallic perovskite with four Os 5d electrons and no sign of magnetism [21]. It has a perfect lattice match with BaTiO₃. Both materials have the same cation, Ba, which will substantially reduce disorder during epitaxial growth. For BaOsO₃/BaTiO₃ we find an electric-field tunable Rashba spin splitting which is at least one magnitude larger than the current experimental record [7–10]. The mechanism behind is nontrivial and summarized in Fig. 1. Substituting BaOsO₃ by BaIrO₃ and BaRuO₃ yields a similar effect; the heterostructure can also be further engineered by varying its thickness and strain.

Method. We mainly focus on a BaOsO₃/BaTiO₃ het-

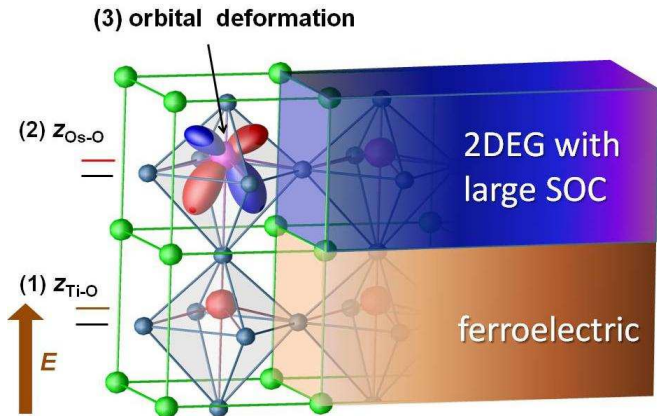


FIG. 1: Schematics of the mechanism behind the giant switchable Rashba effect: (1) An external electric field is amplified and stored as a ferroelectric distortion, in particular Ti-O displacements. (2) These displacements entail, via the oxygen octahedron network of the perovskite heterostructure, Os-O displacements. (3) As a consequence of the Os-O displacements the Os orbitals deform, which reflects the broken inversion symmetry. This orbital deformation and the strong SOC of Os finally lead to a giant Rashba spin splittings that is controllable by an electric-field.

eroheterostructure which has two structural phases: a paraelectric perovskite phase and a distorted ferroelectric phase, see Fig. 2(c) and (d), respectively. We use density-functional theory (DFT) with generalized gradient approximation (GGA) potential [22] in the Vienna Ab initio Simulation Package (VASP) [23, 24] and fully relax all the atomic positions, only fixing the paraelectric or ferroelectric symmetries. At zero temperature, the ferroelectric distorted perovskite has the lower GGA energy, but -as in the bulk- the undistorted paraelectric phase will prevail at elevated temperatures.

Based on the fully relaxed atomic structures, electronic band structures are calculated with modified Becke-Johnson (mBJ) [25] exchange potential as implemented in the Wien2k code [26], which improves the calculated bandgap of BaTiO₃. The SOC is included as a perturbation using the scalar-relativistic eigenfunctions of the valence states. Employing *wien2wannier* [27], we project the Wien2k bandstructure onto maximally localized[28] Wannier orbitals, from which the orbital deformation is analyzed and a realistic tight binding model is derived [29]. We also vary the thickness of the thin films, replace the BaOsO₃ by BaRuO₃ or BaIrO₃, and simulate the strain effect by fixing the in plane lattice constant to the value of a SrTiO₃ substrate. Correlation effects from local Coulomb interaction are studied in the Supplementary Material.

Paraelectric phase. We mainly focus on a BaOsO₃/BaTiO₃ heterostructure, (BaOsO₃)₁/(BaTiO₃)₄, which consists of one BaOsO₃ layer alternating with four BaTiO₃ layers. Bulk BaTiO₃

is a d^0 insulator: the empty Ti 3d states lie about 3eV above occupied O 2p states. Bulk BaOsO₃ is a d^4 metal: four electrons in the Os 5d orbitals of t_{2g} character are 0.8eV above the filled O 2p states. Since BaOsO₃ and BaTiO₃ share oxygen atoms at the interface, the O 2p states align; and the Os 5d states will stay in the energy gap of BaTiO₃. Hence, the density functional theory (DFT) calculated band structures of BaOsO₃/BaTiO₃ in Fig. 2 shows three Os t_{2g} (xy , yz , xz) bands near the Fermi level; they are dispersionless along the z direction (not shown). That is, the low energy electronic degrees of freedom are confined by the insulating BaTiO₃ layers to the OsO₂ plane, forming a 2DEG. Already in the high temperature paraelectric phase, this heterostructure confinement reduces the initial cubic symmetry of the Os t_{2g} orbitals in the bulk perovskite: At Γ the xy band in Fig. 2 (a) is 1.2eV lower in energy than the degenerate yz/xz bands (Fig. 2(a)). Including the SOC, the yz/xz doublet splits into two subbands with mixed yz/xz orbital character, see Fig. 2(b). For the paraelectric phase of Fig. 2(a-c), the spin degeneracy is however still preserved.

To better understand the DFT results, we construct an interface hopping Hamiltonian H_0^i [30] for the 2DEG confined Os t_{2g} electrons by a Wannier projection. The energy-momentum dispersion for the xy orbital is $\epsilon(\mathbf{k})^{xy} = -2t_1 \cos k_x - 2t_1 \cos k_y - 4t_3 \cos k_x \cos k_y$, while that of the yz is $\epsilon(\mathbf{k})^{yz} = -2t_2 \cos k_x - 2t_1 \cos k_y$ ($\epsilon(\mathbf{k})^{xz}$ is symmetrically related by $x \leftrightarrow y$). The largest hopping $t_1 = 0.392\text{eV}$ is along the direction(s) of the orbital lobes, $t_2 = 0.033\text{eV}$ and $t_3 = 0.094\text{eV}$ indicate a much smaller hopping perpendicular to the lobes and along (1, 1, 0), respectively. The xy - yz/xz orbital splitting at Γ is $2t_1 - 2t_2 + 4t_3 = 1.1\text{eV}$ and arises from the anisotropy of the orbitals. Overall, the three parameter tight binding model in Fig. 3(a) (dashed line) is consistent with DFT in Fig. 2(a). Next, we include the atomic SOC Hamiltonian $H_\xi = \xi \vec{l} \cdot \vec{s}$, expressed in the t_{2g} basis with $\xi = 0.44\text{eV}$ for Os. It lifts the yz/xz degeneracy and yields good agreement with DFT, cf. Fig. 3(a) (solid line) and Fig. 2(b).

Ferroelectric phase. In sharp contrast to the paraelectric case, ferroelectrically distorted BaOsO₃/BaTiO₃ exhibits evident spin splittings in the presence of SOC, see Fig. 2(f). Note, in the absence of SOC the DFT band structure in Fig. 2(e) is still very similar to the paraelectric case in Fig. 2(a). The spin splitting E_R^{xy} of the xy band is small around Γ , but strongly enhanced up to 50meV around the xy/yz crossing region as shown in Fig. 2(g), cf. Table I, . The other two subbands of yz/xz character also show a strong splitting around Γ . In this respect, the upper yz/xz subband exhibits a standard Rashba behavior, see the magnification in Fig. 2(h), where the momentum offset $k_0 = 0.043 \text{ \AA}^{-1}$, the Rashba energy $E_R = 4 \text{ meV}$, and hence $\alpha_R = 2E_R/k_0 = 0.186 \text{ eV \AA}$. The behavior of the lower

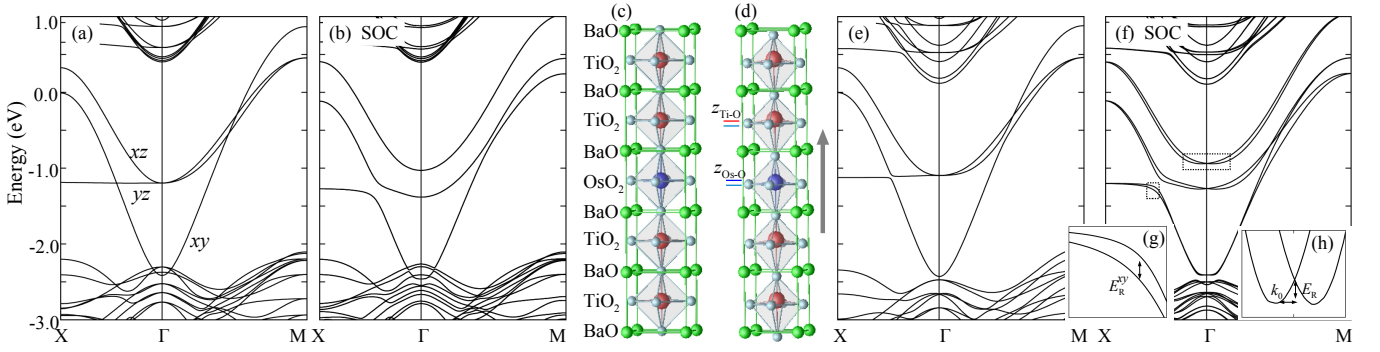


FIG. 2: DFT calculated band structures of $(\text{BaOsO}_3)_1/(\text{BaTiO}_3)_4$ multilayers for the paraelectric (c) and ferroelectric structure (d). The paraelectric heterostructure breaks cubic but not inversion symmetry so that the Os xy orbital splits off from two degenerate yz/xz orbitals without SOC (a); including SOC further lifts the yz/xz degeneracy (b). The ferroelectric state further breaks inversion symmetry, which essentially does not change the bandstructure in the absence of SOC (e) but leads to substantial spin splittings in the presence of SOC (f). The spin splitting E_R^{xy} at the $xy - yz$ crossing region is magnified in (g), while the standard Rashba spin splitting E_R with momentum offset k_0 around Γ of the upper yz/xz mixed orbital is magnified in (h).

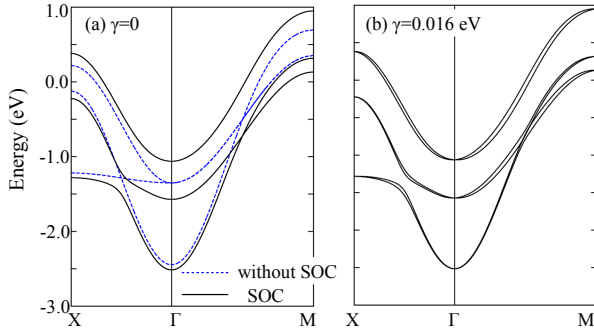


FIG. 3: Tight binding bandstructure of the three Os t_{2g} orbitals for (a) the paraelectric case with and without SOC and (b) the ferroelectric case with SOC and asymmetry parameter $\gamma = 0.016$ eV taken from the Wannier projection.

yz/xz subband is more complex (distorted) due to the proximity of the crossing region.

These spin splittings from ferroelectric distortions which break the inversion symmetry. Bulk BaOsO_3 has no such ferroelectric distortions and is inversion symmetric with Os and O atom in the same plane. Also for the paraelectric heterostructure, the OsO_2 layer is still an inversion plane. The ferroelectric heterostructure breaks inversion symmetry. As listed in Table I, the averaged ferroelectric Ti-O displacement in BaTiO_3 layers is around 0.14 Å, which efficiently induces a sizable Os-O displacement of 0.05 Å via the oxygen octahedron network of the perovskite structure. This structural distortion modifies the crystal environment of Os t_{2g} orbitals and deforms the orbital lobes, see Fig. 1.

In order to quantify the orbital deformation, we project the DFT results above onto maximally localized Wannier orbitals and directly extract the key parameter: a directional, spin-independent inter-orbital hopping $\gamma = \langle xy|H|yz(R)\rangle$, where R is the nearest neighbor in x direc-

tion. In \mathbf{k} -space one gets as a matrix for the yz, xz, xy orbitals (independent of spin) [29]

$$H_\gamma = \gamma \begin{pmatrix} 0 & 0 & 2i \sin k_x \\ 0 & 0 & 2i \sin k_y \\ -2i \sin k_x & -2i \sin k_y & 0 \end{pmatrix}.$$

We obtain $\gamma = 0.016$ eV for the ferroelectric heterostructure, while for the paraelectric case $\gamma = 0$ due to inversion symmetry. Let us emphasize that γ is the relevant measure for the orbital deformation and inversion symmetry breaking. In combination with the strong SOC of OS $5d$ electrons, H_γ results in the present giant Rashba spin splitting.

The Hamiltonian $H_0^i + H_\xi + H_\gamma$ already well describes the spin splittings of the xy orbital in good agreement with DFT results, but underestimates the spin splittings of the yz/xz subbands near Γ . The reason for this is that the atomic SOC is not an accurate description anymore because the SOC of Os is too strong and the deviation from the inversion symmetry too large. Hence, we need to go beyond the purely atomic SOC and include an inversion asymmetry correction to the SOC matrix so that H_ξ in the t_{2g} basis ($yz|\uparrow\rangle, yz|\downarrow\rangle, xz|\uparrow\rangle, xz|\downarrow\rangle, xy|\uparrow\rangle, xy|\downarrow\rangle$) reads

$$\begin{pmatrix} 0 & 2\gamma' \sin k_y & i\frac{\xi}{2} & 0 & 0 & -\frac{\xi}{2} \\ 2\gamma' \sin k_y & 0 & 0 & -i\frac{\xi}{2} & \frac{\xi}{2} & 0 \\ -i\frac{\xi}{2} & 0 & 0 & -2\gamma' \sin k_x & 0 & i\frac{\xi}{2} \\ 0 & i\frac{\xi}{2} & -2\gamma' \sin k_x & 0 & i\frac{\xi}{2} & 0 \\ 0 & \frac{\xi}{2} & 0 & -i\frac{\xi}{2} & 0 & 0 \\ -\frac{\xi}{2} & 0 & -i\frac{\xi}{2} & 0 & 0 & 0 \end{pmatrix}.$$

For the bandstructure of Fig. 3(b) we have taken $\gamma' = 0.022$ eV from the Wannier projection, yielding good agreement with the DFT results Fig. 2(f).

TABLE I: Polar distortions and Rashba spin splittings of $(\text{BaOsO}_3)_n/(\text{BaTiO}_3)_m$ multilayers, alternating n layers of BaOsO_3 and m layers of BaTiO_3 . Second and third column: averaged displacement of Os-O and Ti-O along z as calculated by DFT. Forth column: strength of the interface asymmetry term γ obtained from the Wannier projection. Fifth to seventh column: DFT calculated parameters characterizing Rashba effects: momentum offset k_0 , Rashba energy E_R , and Rashba coefficient α_R of the upper yz/xz subband around Γ as defined in Fig. 2(h). Eighth column: spin splitting E_R^{xy} around the crossing region of xy and yz orbitals as in Fig. 1(g). To demonstrate the effects of heterostructure engineering, we also list the results of $\text{BaOsO}_3/\text{BaTiO}_3$ strained by a SrTiO_3 substrate, as well as $\text{BaRuO}_3/\text{BaTiO}_3$ and $\text{BaIrO}_3/\text{BaTiO}_3$. Band structures are given in Supplementary Material.

$n : m$	Os-O (\AA)	Ti-O (\AA)	γ (eV)	k_0 (\AA^{-1})	E_R (eV)	α_R (eV \AA)	E_R^{xy} (eV)
1:3 $\text{BaOsO}_3/\text{BaTiO}_3$	0.038	0.065	0.011	0.025	0.001	0.08	0.031
1:4	0.049	0.103	0.016	0.043	0.004	0.186	0.053
2:3	<0.010	<0.010	0.003	0	0	-	0.004
2:4	0.024	0.071	0.010	0.035	0.002	0.114	0.018
1:3 strained	0.095	0.223	0.030	0.105	0.021	0.396	0.102
1:4 strained	0.099	0.229	0.031	0.115	0.024	0.417	0.106
1:4 $\text{BaIrO}_3/\text{BaTiO}_3$	0.115	0.119	0.021	0.145	0.053	0.731	0.051
1:4 $\text{BaRuO}_3/\text{BaTiO}_3$	0.082	0.119	0.015	0.128	0.016	0.250	0.007

Electric-field tunability. The Rashba spin splittings can be tuned by an electric field because of the ferroelectricity of BaTiO_3 . It is a nature of ferroelectrics that an external electric field can tune and even reverse the polarization and structural distortion [17, 20, 31–33], including that of the BaOsO_3 layer. Because of the BaOsO_3 layer, the ferroelectricity of the heterostructure is not as strong as in bulk BaTiO_3 . Hence a smaller electric field change than in the bulk ($E=10^3\text{V/cm}$ [33]) is needed for going through the ferroelectric hysteresis loop. Such an electric field can tune the Rashba coefficient listed in Table I, which are at least one order of magnitude more larger than in semiconductors [7] or $3d$ oxide heterostructures [8–10]. For applications it is of particular importance that E_R now clearly exceeds 0.025 eV, the thermal energy at room temperature. Furthermore, we propose to take advantage of the ferroelectric hysteresis and the remnant ferroelectric polarization, using our heterostructure as a spintronics memory device.

Heterostructure engineering. Besides applying an electric field, heterostructure engineering such as varying its thickness, strain, and the material combination is a powerful way to tune the Rashba spin splittings. First, we vary the thickness of BaOsO_3 and BaTiO_3 . It is well known experimentally and theoretically [20, 34] that below a few nanometer thickness of the BaTiO_3 film, the Ti-O displacement is reduced and eventually ferroelectricity vanishes. As shown in Table I, when decreasing the thickness of BaTiO_3 and increasing that of BaOsO_3 , the Rashba spin splittings is indeed substantially reduced. Second, ferroelectricity of BaTiO_3 is sensitive to strain [35]. Taking SrTiO_3 as a substrate provides a 2.5% in-plane compressive strain. This enhances the ferroelectric distortion as well as Rashba spin splitting, $\alpha_R=0.417\text{eV}\text{\AA}$ in Table I. Given the giant Rashba splitting, photoemission and transport measurements should be able to validate this effect by comparing thin films with different

thickness and substrate. Third, we replace Os by other $5d$ elements for shifting the Fermi energy; and also since some Os oxides are toxic. Indeed, similar physics can be found in $\text{BaIrO}_3/\text{BaTiO}_3$ with $\alpha_R = 0.731\text{eV}\text{\AA}$, see Table I, and in $\text{BaRuO}_3/\text{BaTiO}_3$. The latter also offers a platform to study the interplay of Rashba physics and electronic correlations; for instance, novel phenomena is expected in mixed $3d$ - $5d$ transition-metal materials [36]. Note a strong temperature dependence of the α_R in SrIrO_3 was recently reported [37].

Conclusion. We propose to combine a heavy $5d$ compound such as BaOsO_3 and a ferroelectric such as BaTiO_3 in a heterostructure for realizing giant Rashba spin splittings that are switchable by an electric field. The physics behind is that ferroelectric BaTiO_3 amplifies the electric field through a distortion (polarization) of its TiO_6 octahedra. This distortion very efficiently propagates to the OsO_6 octahedron via the shared oxygens, breaking inversion symmetry and deforming the Os orbital lobes. Together with the strong SOC it leads to a giant tunable Rashba effect with, e.g., $\alpha_R=0.731\text{eV}\text{\AA}$ for $\text{BaIrO}_3/\text{BaTiO}_3$. This is at least one magnitude larger than state-of-the-art. Moreover, the ferroelectric hysteresis and remnant polarization leads to a memory effect which can be exploited for spintronics memory devices.

Acknowledgments. ZZ acknowledges financial support by the Austrian Science Fund through the SFB Vi-CoM F4103-N13, QFZ by NSFC (11204265), the NSF of Jiangsu Province (BK2012248), KH by the European Research Council under the European Union’s Seventh Framework Program (FP/2007-2013)/ERC through grant agreement n. 306447, and WY by the U.S. Department of Energy under Contract No. DE-AC02-98CH10886. Calculations have been done on the Vienna Scientific Cluster (VSC).

-
- [1] I. Žutić, J. Fabian, and S. Das Sarma, *Rev. Mod. Phys.* **76**, 323 (2004).
- [2] S. Datta and B. Das, *Appl. Phys. Lett.* **56**, 665 (1990).
- [3] E. I. Rashba, *Sov. Phys. Solid State* **2**, 1109 (1960).
- [4] R. Winkler, *Spin Orbit Coupling Effects in Two-Dimensional Electron and Hole Systems* (Springer, 2003).
- [5] S. LaShell, B. A. McDougall, and E. Jensen, *Phys. Rev. Lett.* **77**, 3419 (1996).
- [6] C. R. Ast, J. Henk, A. Ernst, L. Moreschini, M. C. Falub, D. Pacilé, P. Bruno, K. Kern, and M. Grioni, *Phys. Rev. Lett.* **98**, 186807 (2007).
- [7] J. Nitta, T. Akazaki, H. Takayanagi, and T. Enoki, *Phys. Rev. Lett.* **78**, 1335 (1997).
- [8] A. D. Caviglia, M. Gabay, S. Gariglio, N. Reyren, C. Cancellieri, and J.-M. Triscone, *Phys. Rev. Lett.* **104**, 126803 (2010).
- [9] M. Ben Shalom, M. Sachs, D. Rakhmilevitch, A. Palevski, and Y. Dagan, *Phys. Rev. Lett.* **104**, 126802 (2010).
- [10] H. Nakamura, T. Koga, and T. Kimura, *Phys. Rev. Lett.* **108**, 206601 (2012).
- [11] P. D. C. King, R. C. Hatch, M. Bianchi, R. Ovsyannikov, C. Lupulescu, G. Landolt, B. Slomski, J. H. Dil, D. Guan, J. L. Mi, et al., *Phys. Rev. Lett.* **107**, 096802 (2011).
- [12] P. D. C. King, R. H. He, T. Eknapakul, P. Buaphet, S.-K. Mo, Y. Kaneko, S. Harashima, Y. Hikita, M. S. Bahramy, C. Bell, et al., *Phys. Rev. Lett.* **108**, 117602 (2012).
- [13] K. Ishizaka, M. S. Bahramy, H. Murakawa, M. Sakano, T. Shimojima, T. Sonobe, K. Koizumi, S. Shin, H. Miyahara, A. Kimura, et al., *Nat. Mat.* **10**, 521 (2011).
- [14] M. Bahramy, B. Yang, R. Arita, and N. Nagaosa, *Nat. Commun.* **3**, 679 (2012).
- [15] S. Nakosai, Y. Tanaka, and N. Nagaosa, *Phys. Rev. Lett.* **108**, 147003 (2012).
- [16] T. Das and A. V. Balatsky, *Nat. Commun.* **4**, 1972 (2013).
- [17] H. Mirhosseini, I. V. Maznichenko, S. Abdelouahed, S. Ostanin, A. Ernst, I. Mertig, and J. Henk, *Phys. Rev. B* **81**, 073406 (2010).
- [18] J.-J. Zhou, W. Feng, Y. Zhang, and S. A. Y. and Yugui Yao, *Scientific Reports* **4**, 3841 (2014).
- [19] D. Di Sante, P. Barone, R. Bertacco, and S. Picozzi, *Advanced Materials* **25**, 509 (2013), ISSN 1521-4095.
- [20] M. Dawber, K. M. Rabe, and J. F. Scott, *Rev. Mod. Phys.* **77**, 1083 (2005).
- [21] Y. Shi, Y. Guo, Y. Shirako, W. Yi, X. Wang, A. A. Belik, Y. Matsushita, H. L. Feng, Y. Tsujimoto, M. Arai, et al., *Journal of the American Chemical Society* **135**, 16507 (2013).
- [22] J. P. Perdew, K. Burke, and M. Ernzerhof, *Phys. Rev. Lett.* **77**, 3865 (1996).
- [23] G. Kresse and J. Hafner, *Phys. Rev. B* **47**, 558 (1993).
- [24] G. Kresse and J. Furthmüller, *Phys. Rev. B* **54**, 11169 (1996).
- [25] F. Tran and P. Blaha, *Phys. Rev. Lett.* **102**, 226401 (2009).
- [26] P. Blaha, K. Schwarz, G. K. H. Madsen, D. Kvasnicka, and J. Luitz, *WIEN2k, An Augmented Plane Wave + Local Orbitals Program for Calculating Crystal Properties* (Karlheinz Schwarz, Techn. Universität Wien, Austria, 2001), ISBN 3-9501031-1-2.
- [27] J. Kune, R. Arita, P. Wissgott, A. Toschi, H. Ikeda, and K. Held, *Computer Physics Communications* **181**, 1888 (2010), ISSN 0010-4655.
- [28] A. A. Mostofi, J. R. Yates, Y.-S. Lee, I. Souza, D. Vanderbilt, and N. Marzari, *Computer Physics Communications* **178**, 685 (2008), ISSN 0010-4655.
- [29] Z. Zhong, A. Tóth, and K. Held, *Phys. Rev. B* **87**, 161102 (2013).
- [30] Z. Zhong, Q. Zhang, and K. Held, *Phys. Rev. B* **88**, 125401 (2013).
- [31] S. Mathews, R. Ramesh, T. Venkatesan, and J. Benedetto, *Science* **276**, 238 (1997).
- [32] C.-G. Duan, S. S. Jaswal, and E. Y. Tsybal, *Phys. Rev. Lett.* **97**, 047201 (2006).
- [33] R. Tazaki, D. Fu, M. Itoh, M. Daimon, and S. ya Koshihara, *J. Phys.: Condens. Matter.* **21**, 215903 (2009).
- [34] J. Junquera and P. Ghosez, *Nature* **422**, 506 (2003).
- [35] K. J. Choi, M. Biegalski, Y. L. Li, A. Sharan, J. Schubert, R. Uecker, P. Reiche, Y. B. Chen, X. Q. Pan, V. Gopalan, et al., *Science* **306**, 1005 (2004).
- [36] W.-G. Yin, X. Liu, A. M. Tselik, M. P. M. Dean, M. H. Upton, J. Kim, D. Casa, A. Said, T. Gog, T. F. Qi, et al., *Phys. Rev. Lett.* **111**, 057202 (2013).
- [37] L. Zhang, Y. B. Chen, J. Zhou, S.-T. Zhang, Z. bin Gu, S.-H. Yao, and Y.-F. Chen, *arXiv* **1309.7566** (2013).